

Analysis of Parametric Oscillatory Instability in Signal Recycled LIGO Interferometer

V. B. Braginsky, A. Gurkovsky, S. E. Strigin and S. P. Vyatchanin

Faculty of Physics, Moscow State University,

Moscow 119992, Russia,

e-mail: svyatchanin@phys.msu.su

(Dated: February 5, 2018)

We present the analysis of undesirable effect of parametric oscillatory instability in signal recycled LIGO interferometer. The basis for this effect is the excitation of the additional (Stokes) optical mode, with frequency ω_1 , and the mirror elastic mode, with frequency ω_m , when optical energy stored in the main FP cavity mode, with frequency ω_0 , exceeds the certain threshold and the frequencies are related as $\omega_0 \simeq \omega_1 + \omega_m$. We show that possibility of parametric instability in this interferometer is relatively small due to stronger sensitivity to detuning. We propose to “scan” the frequency range where parametric instability may take place varying the position of signal recycling mirror.

I. INTRODUCTION

The full scale terrestrial interferometric gravitational wave antennae LIGO are working now and have sensitivity, expressed in terms of the metric perturbation amplitude, only 2 or 3 times worse than the planned level of $h \simeq 1 \times 10^{-21}$ [1, 2] (see current sensitivity curve in [3]). In Advanced LIGO (to be realized in approximately 2012), after the improvement of the isolation from noises in test masses (the mirrors of the 4 km long optical FP cavities) and increasing the optical power circulating in the resonator up to $W \simeq 830$ kW the sensitivity is expected to reach the value of $h \simeq 1 \times 10^{-22}$ [4, 5].

In [6] we have analyzed the undesirable effect of parametric oscillatory instability in the Fabry-Perot (FP) cavity, which may cause a substantial decrease of the antennae sensitivity or even the antenna malfunction. This effect appears above the certain threshold of the optical power W_c circulating in the main mode, when the difference $\omega_0 - \omega_1$ between the frequency ω_0 of the main optical mode and the frequency ω_1 of the idle (Stokes) mode is close to the frequency ω_m of the mirror mechanical degree of freedom. The coupling between these three modes arises due to the ponderomotive pressure of light in the main and Stokes modes and the parametric action of mechanical oscillation on the optical modes. Above the critical value of light power W_c the amplitude of mechanical oscillation rises exponentially as well as optical power in the idle (Stokes) optical mode. However, E. D’Ambrosio and W. Kells have shown [7] that if in the same unidimensional model the anti-Stokes mode (with frequency $\omega_{1a} = \omega_0 + \omega_m$) is taken into account, then the effect of parametric instability will be substantially dumped or even excluded. In [8], we have presented the analysis based on the model of power recycled LIGO interferometer and demonstrated that anti-Stokes mode could not completely suppress the effect of parametric oscillatory instability. As possible “cure” to avoid the parametric instability we have proposed to change the mirror shape and introduce low noise damping [9]. D. Blair with collaborators proposed valuable idea to heat

the test masses in order to vary curvature radii of mirrors in interferometer and hence to control detuning and decrease overlapping factor between optical and acoustic modes [11, 12, 13]. Recently, the parametric instability effect was observed in experiment [10].

It is interesting that the effect of parametric instability is important not only for large scale LIGO interferometer but it was observed also for micro scale whispering gallery optical resonators [14, 15].

In this paper we propose the detail analysis of parametric instability in signal recycled Advanced LIGO interferometer (i.e. with additional signal recycling (SR) mirror) and show that, on the one hand, the parametric instability in this interferometer can appear at low optical power (about several Watts) but, on the other hand, the probability that parametric instability condition will be fulfilled is small due to small relaxation rates of optical modes (about several Hz). We also show that by varying the position of SR mirror one can change the frequency of anti-symmetric optical mode of interferometer and hence to scan the range of frequencies where parametric instability or its precursors may arise.

In section II we derive the parametric instability conditions in signal recycled LIGO interferometer, we discuss these results in section III. The details of calculations we present in Appendices.

II. SIGNAL RECYCLED INTERFEROMETER

We consider the LIGO interferometer with signal recycling (SR) and power recycling (PR) mirrors — see fig. 1 and notations over there. The port E_6 is used for signal detection. Interferometer is pumped via port F_5 . Simplifications are the following:

- Optical losses in all mirrors are absent (notes about generalization for non zero losses are made in the end of Sec. III). Suspension noise in mirrors is also absent.
- Transmittivity of input mirrors and length of both

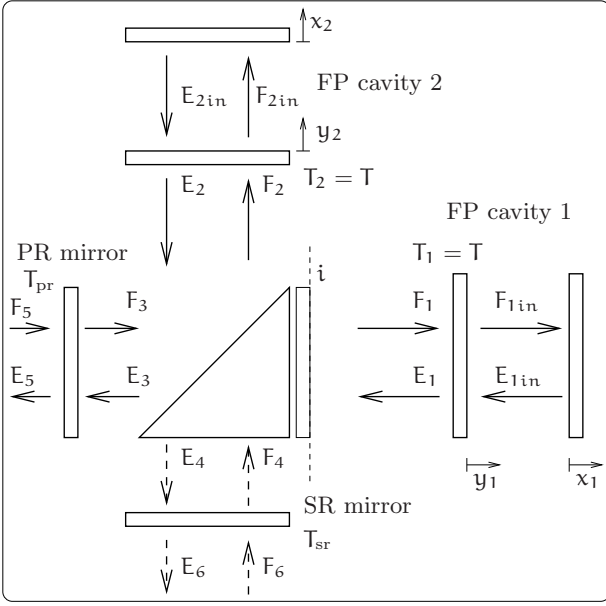


FIG. 1: Signal and power recycled LIGO interferometer. Here F_1 , E_1 are the field amplitudes on the input mirror of the FP cavity 1 (and on plane (i)), F_2 , E_2 are the field amplitudes on the input mirror of the FP cavity 2 and on the beam splitter, F_3 , E_3 , F_4 , E_4 are the field amplitudes on the beam splitter.

FP cavities are the same. They are tuned in resonance with the main mode.

- Optical power W circulating inside the arms of interferometer is constant (approximation of constant field).
- The distances between the input FP mirrors and beam splitter, and between the beam splitter and PR, SR mirrors are short (about several meters) — hence we consider the phase advance of waves traveling between these mirrors as constant and omit its dependence on frequency.

A. FP cavities in arms

We denote the mean amplitude of the wave in the main mode (with frequency ω_0) by cursive capital letters and small fluctuation amplitude of the wave in the Stokes mode (ω_1) by small letters. For example, the electrical field of wave falling on back mirror in FP cavity 1 is the

following:

$$\begin{aligned}
 E(t, \vec{r}_\perp) &\simeq \sqrt{\frac{2\pi}{cS_0}} \mathcal{A}_{0\text{in}}(\vec{r}_\perp) \mathcal{F}_{1\text{in}} e^{-i\omega_0 t} + \\
 &+ \sqrt{\frac{2\pi}{cS_1}} \int_{-\infty}^{\infty} \mathcal{A}_{1\text{in}}(\vec{r}_\perp) f_{1\text{in}}(\Omega) e^{-i(\omega_1 + \Omega)t} \frac{d\Omega}{2\pi} + \\
 &+ \text{h.c.}, \\
 W &= |\mathcal{F}_{1\text{in}}|^2, \\
 S_0 &= \int |\mathcal{A}_{0\text{in}}(\vec{r}_\perp)|^2 d\vec{r}_\perp, \quad S_1 = \int |\mathcal{A}_{1\text{in}}(\vec{r}_\perp)|^2 d\vec{r}_\perp.
 \end{aligned}$$

Here W is the mean power in the main mode circulating inside the cavity, c is the speed of light, dimensionless functions $\mathcal{A}_{0\text{in}}(\vec{r}_\perp)$, $\mathcal{A}_{1\text{in}}(\vec{r}_\perp)$ describe the distributions of optical fields over the beam cross section, integration $\int d\vec{r}_\perp$ is taken over the mirror surface. For simplicity below we consider the distributions of optical fields to be identical at all four mirrors in the arms.

We write down the displacement vector of the elastic mode with eigenfrequency ω_m , for example, for the end mirror of the FP cavity 1 as a product of time and space dependent functions:

$$(x_1(t) e^{-i\omega_m t} + x_1^*(t) e^{i\omega_m t}) \vec{u}(\vec{r})$$

where x_1 and x_1^* are slowly varying amplitudes and \vec{u} is spatial vector of displacements of elastic mode in the mirror.

Here we assume that the input and the end mirrors in the FP cavity 1 are elastically identical (the modes of their elastic oscillations coincide). Then we start from the formulas derived in Appendix A in frequency domain:

$$f_{1\text{in}}(\Omega) = \mathcal{T}_\Omega f_1(\Omega) + \mathcal{F}_{1\text{in}} N_1 \frac{\mathcal{T}_\Omega 2ikz_1^*(\Delta - \Omega)}{i\sqrt{\Gamma}}, \quad (2.1)$$

$$e_1(\Omega) = \mathcal{R}_\Omega f_1(\Omega) - \mathcal{F}_{1\text{in}} N_1 \mathcal{T}_\Omega 2ikz_1^*(\Delta - \Omega), \quad (2.2)$$

$$\mathcal{T}_\Omega = \frac{2i\gamma}{\sqrt{\Gamma}(\gamma - i\Omega)}, \quad \mathcal{R}_\Omega = \frac{\gamma + i\Omega}{\gamma - i\Omega}, \quad (2.3)$$

$$\Delta = \omega_0 - \omega_1 - \omega_m, \quad k = \omega_1/c, \quad (2.4)$$

$$z_1(\Omega) \equiv x_1(\Omega) - y_1(\Omega), \quad \gamma = c\Gamma/4L.$$

Here N_1 is an overlapping factor (A2), L is the distance between the mirrors of the FP cavities in arms. We also omit non-resonance terms ($\sim z_1$). In order to clarify the dependence of $z_1^*(\Delta - \Omega)$ we have to write down the last term in (2.1) in detail and to equate exponential quantities in the left and right parts of (2.1):

$$\begin{aligned}
 \mathcal{F}_{1\text{in}} e^{-i(\omega_0 - \omega_1)t} \frac{\mathcal{T}_\Omega}{i\sqrt{\Gamma}} N_1 \times 2ikz_1^*(\Omega') e^{i(\omega_m + \Omega')t}, \\
 - i\Omega t = -i(\omega_0 - \omega_1)t + i(\omega_m + \Omega')t \rightarrow \Omega' = \Delta - \Omega.
 \end{aligned}$$

For the FP cavity 2 all formulas are the same. For the mean amplitudes we have: $\mathcal{E}_1 = \mathcal{F}_1$, $\mathcal{E}_2 = \mathcal{F}_2$.

B. Beam splitter

We consider that F_3 , E_3 are the field amplitudes on the PR mirror and the beam splitter, and F_4 , E_4 are the field amplitudes on the beam splitter as it is shown in fig. 1. We assume that the beam splitter transparency is $T_{bs} = 1/2$ and the phase of the wave due to traveling between the FP cavity 2 and the beam splitter is $e^{i\phi_2} = 1$, and between the FP cavity 1 and the beam splitter is $e^{i\phi_1} = i$. So we can imagine such plane (see Fig. 1), that phase advance between the beam splitter and this plane is $e^{i\phi_1} = i$ and between this plane and the input mirror of the FP cavity 1 is fold to 2π . Then F_1 , E_1 are the field amplitudes on the input mirror of the FP cavity 1 (and on the plane (i)), F_2 , E_2 are the field amplitudes on the input mirror of the FP cavity 2 and on the beam splitter. For the mean amplitudes we have:

$$\mathcal{F}_1 = -\mathcal{F}_3/\sqrt{2}, \quad \mathcal{F}_2 = -\mathcal{F}_3/\sqrt{2}, \quad \mathcal{E}_4 = 0, \quad \mathcal{E}_3 = \mathcal{F}_3.$$

It is convenient to introduce symmetric and anti-symmetric modes F_{\pm} :

$$F_+ = (F_1 + F_2)/\sqrt{2}, \quad \mathcal{F}_+ = -\mathcal{F}_3, \quad f_+ = -f_3, \quad (2.5)$$

$$F_- = (F_1 - F_2)/\sqrt{2}, \quad \mathcal{F}_- = 0, \quad f_- = -if_4. \quad (2.6)$$

Then for fluctuation fields e_3 and e_4 we have:

$$e_4 = -\mathcal{R}(\Omega)f_4 - \mathcal{F}_{1in} \mathcal{T}_\Omega \sqrt{2} N_1 k z_-^*, \quad (2.7)$$

$$e_3 = \mathcal{R}(\Omega)f_3 + \mathcal{F}_{1in} \mathcal{T}_\Omega \sqrt{2} i N_1 k z_+^*, \quad (2.8)$$

$$z_- = (x_1 - y_1) - (x_2 - y_2), \quad z_+ = (x_1 - y_1) + (x_2 - y_2).$$

We see that symmetric and anti-symmetric modes can be analyzed separately. In subsection II C we consider the symmetric mode which interacts with sum coordinate z_+ and in subsection II D: the anti-symmetric mode interacting with differential coordinate z_- . It is worth to note that such consideration is possible only if all four mirrors in the FP cavities in arms are optically and elastically identical, just as we have assumed. For the opposite case, when the eigenfrequencies of elastic modes are different we can consider elastic mode only in one mirror and assume other mirrors to be fixed (see subsection II E).

C. Power Recycling Mirror and symmetric mode

Assuming that PR cavity is in resonance, we obtain two equations in time domain describing coupling between optical and elastic modes (see details of calculations in Appendix B) :

$$\dot{f}_{in+} + \gamma_{0+} f_{in+} = \frac{i N_1 \mathcal{F}_{1in} \omega_1}{\sqrt{2} L} z_+^* e^{-i\Delta t}, \quad (2.9)$$

$$\dot{z}_+^* + \gamma_m z_+^* \simeq \frac{2\sqrt{2} N_1^* \mathcal{F}_{1in}^*}{\pi i \omega_m m \mu} f_{in+}(t) e^{i\Delta t}. \quad (2.10)$$

Here γ_{0+} is the relaxation rate of symmetric mode (B6), γ_m is the relaxation rate of elastic mode, m is the mass of each of the mirrors, and μ is normalizing constant (A10).

We find the solutions of this set of equations (2.9, 2.10) in the form:

$$f_{in+}(t) = f_{in+} e^{(\lambda - i\Delta)t}, \quad z_+^*(t) = z_+^* e^{\lambda t},$$

and as a result we obtain the characteristic equation:

$$2Q = (\lambda - i\Delta + \gamma_{0+})(\lambda + \gamma_m), \quad (2.11)$$

$$Q \equiv \frac{\Lambda_1 W \omega_1}{c L \omega_m m}, \quad W = |\mathcal{F}_{1in}|^2, \quad (2.12)$$

$$\Lambda_1 \equiv \frac{|N_1|^2}{\mu} = \frac{V \left| \int \mathcal{A}_{0in} \mathcal{A}_{1in}^* \mathbf{u}_\perp d\vec{r}_\perp \right|^2}{\int |\mathcal{A}_{0in}|^2 d\vec{r}_\perp \int |\mathcal{A}_{1in}|^2 d\vec{r}_\perp \int |\vec{u}(\vec{r})|^2 d\vec{r}}. \quad (2.13)$$

Here Λ_1 is general overlapping factor between the main, Stokes optical modes, and elastic mode, \mathbf{u}_\perp is the component of displacement vector \vec{u} of elastic mode normal to the mirror surface, $\int d\vec{r}_\perp$ corresponds to the integration over the mirror surface and $\int d\vec{r}$: to the integration over the mirror volume V .

We present λ as a sum of real and imaginary parts: $\lambda = a + ib$, substitute it into (2.11) and obtain two equations:

$$a^2 - b^2 + a(\gamma_m + \gamma_{0+}) + b\Delta + \gamma_m \gamma_{0+} - 2Q = 0, \quad (2.14)$$

$$2ab + b(\gamma_m + \gamma_{0+}) - a\Delta - \gamma_m \Delta = 0. \quad (2.15)$$

The parametric instability condition corresponds to $a > 0$. Putting $a = 0$ we find the condition of boundary situation (between stability and instability). The additional analysis gives the sign of inequality in the parametric instability condition. We find formal solution for b from (2.15) with assumption $a = 0$, substitute it into (2.14), and obtain the parametric instability condition:

$$\frac{2Q}{\gamma_m \gamma_{0+}} > 1 + \frac{\Delta^2}{(\gamma_m + \gamma_{0+})^2}. \quad (2.16)$$

This condition can be compared with the condition of parametric instability for single FP cavity [6] with relaxation rate γ

$$\mathcal{R}_0 > 1 + \frac{\Delta^2}{\gamma^2}, \quad \mathcal{R}_0 = \frac{Q}{\gamma_m \gamma}. \quad (2.17)$$

We see that conditions (2.16) and (2.17) approximately coincide with each other if one substitutes γ_{0+} instead of γ and takes into account inequality $\gamma_m \ll \gamma_{0+}$ (see estimates in Appendix E). The factor 2 appears due to the fact that in derivation (2.16) we take into account the displacements of 4 mirrors in the interferometer while in (2.17) the displacement of only one mirror of FP cavity is taken into account.

D. Signal recycling mirror and anti-symmetric mode

We assume that in general case the SR cavity is not in resonance and phase advance ϕ of the wave between the SR mirror and the beam splitter is an arbitrary one. We also assume that ϕ does not depend on frequency Ω due to the short length of the SR cavity. After the calculations presented in Appendix C one can obtain two equations describing the coupling between optical and elastic modes:

$$\dot{f}_{\text{in-}} + (\gamma_{0-} - i\delta) f_{\text{in-}} = \frac{N_1 \mathcal{F}_{1\text{in}} i \omega_1 z_-^*}{L\sqrt{2}} e^{i\Delta t}, \quad (2.18)$$

$$\dot{z}_-^* + \gamma_m z_-^* \simeq \frac{2\sqrt{2} N_1^* \mathcal{F}_{1\text{in}}^*}{\pi i \omega_m m \mu} f_{\text{in-}}(t) e^{i\Delta t}. \quad (2.19)$$

Here γ_{0-} is the relaxation rate of anti-symmetric mode (C6), δ is the detuning depending on the SR mirror position (C5).

Searching for the solution of the equations set (2.18, 2.19) in the form:

$$f_{\text{in-}}(t) = f_{\text{in-}} e^{(\lambda - i\Delta)t}, \quad z_-^*(t) = z_-^* e^{\lambda t},$$

we obtain the characteristic equation:

$$2Q = (\lambda + \gamma_{0-} - i(\delta + \Delta))(\lambda + \gamma_m). \quad (2.20)$$

We see that the characteristic equation (2.20) differs from the analogous one for the symmetric mode (2.11) only by replacement of $\Delta \rightarrow \Delta + \delta$. Hence we can write down the condition of instability for the anti-symmetric mode using (2.16):

$$\frac{2Q}{\gamma_m \gamma_{0-}} > 1 + \frac{(\Delta + \delta)^2}{(\gamma_m + \gamma_{0-})^2}. \quad (2.21)$$

The relaxation rate γ_{0-} and detuning δ depend on angle ϕ (the position of the SR mirror). Analyzing definitions (C6, C5) we see that there are two cases: close to resonance (ϕ close to 0) and to anti-resonance (ϕ is close to $\pi/2$) cases. Expanding the denominator in (C6, C5) in series over T_{sr} (recall $T_{\text{sr}} \ll 1$), we obtain useful formulas:

$$\delta \simeq \frac{\gamma \sin 2\phi}{\frac{T_{\text{sr}}^2}{8} + \cos^2 \phi \left(2 - T_{\text{sr}} - \frac{T_{\text{sr}}^2}{4} \right)}, \quad (2.22)$$

$$\gamma_{0-} \simeq \frac{\gamma T_{\text{sr}}}{\frac{T_{\text{sr}}^2}{4} + 2 \cos^2 \phi \left(2 - T_{\text{sr}} - \frac{T_{\text{sr}}^2}{4} \right)}. \quad (2.23)$$

Manipulating the angle ϕ (via the SR mirror position variation) we can vary the relaxation rate γ_{0-} and detuning δ in wide ranges:

$$\frac{T_{\text{sr}} \gamma}{4} \leq \gamma_{0-} \leq \frac{4\gamma}{T_{\text{sr}}}, \quad \frac{-2\gamma}{T_{\text{sr}}} \leq \delta \leq \frac{2\gamma}{T_{\text{sr}}}. \quad (2.24)$$

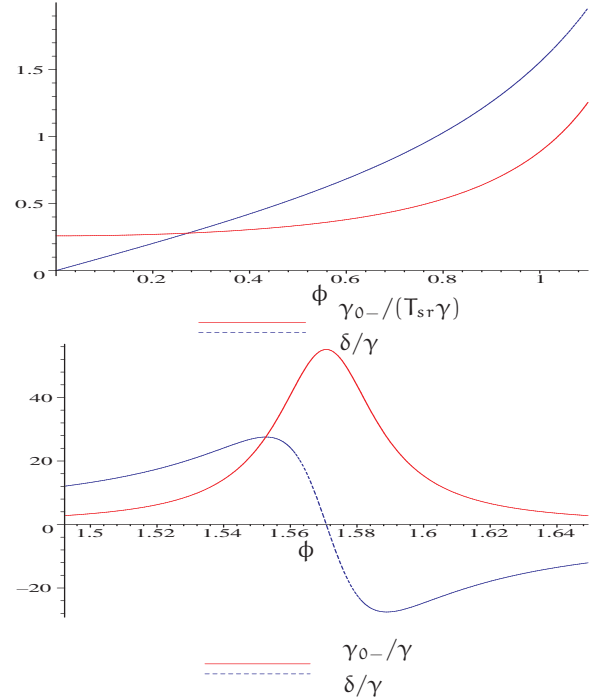


FIG. 2: Dependence of the relaxation rate γ_{0-} and detuning δ of anti-symmetric mode on angle ϕ for $T_{\text{sr}} = 0.07$ (planned in Advanced LIGO). Top: close to resonance case. Bottom: close to anti-resonance case.

It is demonstrated in Fig. 2. (Note that the above formula is valid only while $\gamma_{0-} \ll c/L$, *i.e.* $T/8T_{\text{sr}} \ll 1$.) Using formula (2.24), we have the following estimates for parameters of Advanced LIGO (Appendix E):

$$1.6 \text{ sec}^{-1} \leq \gamma_{0-} \leq 6 \times 10^3 \text{ sec}^{-1}, \\ -3 \times 10^3 \text{ sec}^{-1} \leq \delta \leq 3 \times 10^3 \text{ sec}^{-1}.$$

So we can “scan” the frequency range to find instability (or its precursors) by variation of the SR mirror position. As precursors we may register Stokes modes providing information about the resonance frequencies of elastic modes which “suit” each other by spatial distributions. These Stokes modes may be the modes of higher orders (dipole, quadrupole and so on). In order to extract them one has to detune the output mode cleaner which is planned to be placed after the SR mirror which is an additional but not complicated operation¹. It provides us *in situ* with very valuable information about the possible danger of parametric instability.

¹ Advanced LIGO currently plans a rigid short (tens of cm) output mode cleaner which can be put on resonance for the carrier but which rejects all frequencies out of mode cleaner bandwidth. Detuning, for example, to dipole mode requires change of mode cleaner length ℓ by relatively small value $\delta\ell/\ell = (\omega_{\text{dipole}} - \omega_{\text{main}})/\omega_{\text{main}} \simeq 10^{-7}$.

E. Different mirrors: only one mirror is in resonance

Here we consider the case when the frequencies of elastic modes in different mirrors do not coincide with each other and thus, we assume that the frequency of elastic mode of only one mirror is in resonance, for example, the end mirror in the FP cavity 1. Therefore we consider other mirrors as fixed, and only the coordinate x_1 will be taken into account. Then Eqs. (2.9, 2.18) will be valid with substitution $x_1 \rightarrow z_+, z_-$. For calculation of ponderomotive force we consider the field in the FP cavity 1 as a sum of symmetric and anti-symmetric modes fields. After calculations presented in Appendix D we get the characteristic equation in the compact form:

$$(\lambda + i\Delta + \gamma_m) = \frac{Q}{2} \left(\frac{1}{\lambda + \gamma_{0+}} + \frac{1}{\lambda - i\delta + \gamma_{0-}} \right). \quad (2.25)$$

Instability condition in pure power recycled LIGO interferometer. Using characteristic equation (2.25) we consider the case when there is no SR mirror in the interferometer, then we have to substitute $T_{sr} = 1$ into (C5,C6) and hence $\delta = 0$, $\gamma_{0-} = \gamma$ (γ is the relaxation rate of a single FP cavity in arm). For such power recycled configuration we have the following inequalities:

$$\gamma_m \ll \gamma_{0+} \ll \gamma. \quad (2.26)$$

The analysis presented in Appendix D gives the following parametric instability condition:

$$\frac{Q}{2\gamma_m} \left(\frac{\gamma_{0+}}{\gamma_{0+}^2 + \Delta^2} + \frac{\gamma}{\gamma^2 + \Delta^2} \right) \geq 1. \quad (2.27)$$

It is useful to rewrite approximation of this instability condition in particular cases for different detunings Δ :

$$\Delta \ll \gamma_{0+} : \quad \frac{Q}{2\gamma_m \gamma_{0+}} \geq 1, \quad (2.28a)$$

$$\gamma_{0+} \ll \Delta \ll \gamma : \quad \frac{Q}{2\gamma_m \gamma} \left(\frac{\gamma_{0+} + \gamma}{\Delta^2} + 1 \right) \geq 1, \quad (2.28b)$$

$$\Delta \gg \gamma : \quad \frac{Q\gamma}{2\gamma_m \Delta^2} \geq 1. \quad (2.28c)$$

Note that condition (2.27) *slightly differs* from the formula (6) in our paper [8]². However, the error made in [8] is insignificant: the particular cases (2.28) *coincide* with analogous particular cases obtained from formula (6) in [8].

² Our notations relate to the notations in [8] as follows: $\gamma \Rightarrow \delta_1$, $\gamma_{0+} \Rightarrow \delta_{pr}$, $\gamma_m \Rightarrow \delta_m$, and parameters Q and \mathcal{R}_0 relate as (2.17).

The instability condition for signal recycled LIGO interferometer. Using estimates of Appendix E we have the inequality

$$\gamma_m \ll \gamma_{0+} < \gamma_{0-}. \quad (2.29)$$

From the characteristic equation (2.25) and inequality (2.29) we obtain the parametric instability condition:

$$\frac{Q}{2\gamma_m} \left(\frac{\gamma_{0+}}{\gamma_{0+}^2 + \Delta^2} + \frac{\gamma_{0-}}{\gamma_{0-}^2 + (\Delta + \delta)^2} \right) > 1. \quad (2.30)$$

See details of calculations in Appendix D.

III. DISCUSSION

For our discussion we use the following scale of relaxations rates (see Appendix E): the relaxation rate of elastic mode $\gamma_m \simeq 6 \times (10^{-4} \div 10^{-2}) \text{ sec}^{-1}$, the relaxation rates of symmetric and anti-symmetric modes $\gamma_{0+} \simeq 1.5 \text{ sec}^{-1}$, $\gamma_{0-} \geq 2 \text{ sec}^{-1}$, and the relaxation rate of a single FP cavity in arm $\gamma \simeq 100 \text{ sec}^{-1}$.

First of all we see that the main difference between the parametric instability in a signal recycled Advanced LIGO interferometer and in pure power recycled interferometer is the crucial dependence on detuning, compare Eqs. (2.16,2.21,2.30) with (2.27). In power recycled interferometer the parametric instability takes place if $|\Delta| < \gamma \simeq 100 \text{ sec}^{-1}$ while in signal recycled interferometer: $|\Delta| < \gamma_{0+}$, $\gamma_{0-} \simeq 2 \text{ sec}^{-1}$.

On the one hand, in case of relatively small detuning the parametric instability in a signal recycled interferometer takes place at relatively low value of optical power. For example, if $\Delta \ll \gamma_{0+}$ and $\delta \gg \gamma_{0-}$ one can obtain from Eq. (2.30) that the parametric instability will take place at power $W_c \simeq 5 \text{ W}$ (!) circulating in arms (if $\omega_m = 10^5 \text{ sec}^{-1}$, $\gamma_m = 6 \times 10^{-4} \text{ sec}^{-1}$, $\Lambda_1 \simeq 1$). On the other hand, there is a small chance that such small detuning will take place and for large detuning ($|\Delta| > \gamma_{0+}$) the realization of parametric instability requires dramatically larger optical power: $W_c \sim \Delta^2 / \gamma_{0+}^2$. For example, if detuning is about 1 kHz ($|\Delta| \simeq 6 \times 10^3 \text{ sec}^{-1}$) and other parameters are the same one can obtain $W_c \simeq 10^8 \text{ W}$ (!). For the same reason the possibility that the presence of anti-Stokes mode can depress the parametric instability is small enough especially for such detunings. Therefore, we did not consider the anti-Stokes mode in our analysis (“anti-Stokes” generalization can be done using the same approach as in [8]).

Another factor that can decrease the possibility of parametric instability is the small value of overlapping factor; even if the frequencies of Stokes and elastic modes “suit” each other their spatial distributions (at mirrors surface) may considerably decrease the overlapping factor Λ_1 and, hence, the possibility of parametric instability.

The elastic modes can be calculated numerically. Unfortunately, the numerical calculations of elastic modes

of cylinder mirrors face with obvious difficulty: the accuracy of elastic mode frequencies calculations is dramatically insufficient. The standard packages FEMLAB or ANSYS, used for this purpose [8, 11], provide the accuracy about *several percents* only, while we need the accuracy at least $\gamma_{0+}/\omega_m \simeq 10^{-7} \div 10^{-5}$ (!). Nevertheless, numerical calculations have sense for estimates of overlapping factors and as information (about the frequency range) for the experimentalist where the parametric instability may occur.

Even if the numerical calculation methods will be improved to the extent that they will achieve the required accuracy, they can not solve the problem completely because: (i) the shape of mirrors differs from the cylinder shape, for example, the pins to attach suspension fiber may produce the shift of elastic mode frequency up to 100 sec^{-1} [8] and (ii) the inhomogeneity of fused silica (the material mirrors should be manufactured of) may also provide an uncontrollable shift of elastic mode frequency [8]. That is why we present the separate consideration of the case when the elastic mode of only one mirror is taken into account in subsection II E.

Parametric instability can also be investigated in GEO600 configuration interferometer which also has signal and power recycling mirrors, but has no FP cavities in arms. Hence the formulas above can be generalized for GEO600 configuration by putting the transmittance of input mirrors in arms to be equal to 1 and, hence, $\gamma = c/2L$. Then the relaxation rate of symmetric mode will be about $\gamma_{0+}^{\text{GEO}} \simeq T_{\text{pr}}c/4L \simeq 0.75 \times 10^{-5} \text{ sec}^{-1}$ (we assume $T_{\text{pr}} = 0.012$, $L = 1.2 \text{ km}$) and using formula (2.16) we estimate that parametric instability may take place at relatively small optical power $W_c^{\text{GEO}} \simeq 100 \text{ W}$ circulating in arms if we assume zero detuning $\Delta = 0$, $m = 10 \text{ kg}$, $\omega_m = 10^4 \text{ sec}^{-1}$, $\gamma_m = 10^{-4} \text{ sec}^{-1}$ and $\Lambda_1 = 1$.

Our consideration can be generalized for the case of mirrors with losses. Let each mirrors in the FP cavity to have loss coefficient A which is small compared to transparency: $\eta \equiv 2A/T < 1$. In this case all formulas (2.16, 2.21, 2.27, 2.30) for parametric instability conditions are valid with the following substitutions:

$$\gamma \Rightarrow \gamma(1 + \eta), \quad \gamma_{0\pm} \Rightarrow \gamma_{0\pm} + \eta\gamma. \quad (3.1)$$

For Advanced LIGO the losses in mirrors are small enough (it is planned that $A \simeq 5 \text{ ppm}$, $\eta \simeq 2 \times 10^{-3}$).

However, the diffractive losses may be large for optical modes with high indices [8]. Kip Thorne [16, 17] pointed out that the case of large diffractive losses (when round trip relative losses are close to unity) requires a separate analysis. This work is in progress now [18].

Conclusion

We have shown that in the signal recycled Advanced LIGO interferometer the possibility of falling into the

trap of the parametric instability is smaller than for the pure power recycled one due to stronger sensitivity to detuning.

We think that the most reliable method to avoid the parametric instability is the *direct experimental* test. For signal recycled interferometer we have good method to investigate the possibility of parametric instability experimentally *in situ*: varying the SR mirror position, one can detune the frequency of anti-symmetric mode in wide range to find the instability or its precursors as it was shown in subsection II D. It is important that for GEO600 configuration we can introduce detuning larger than in Advanced LIGO: the scanning may be performed inside the free spectral range $c/2L$. This scanning combined with the detailed knowledge about the elastic modes (it can be obtained *in situ* in separate experiments before the test masses are placed into the interferometer) will provide us with very valuable information helpful for avoiding the parametric instability.

We hope that parametric instability effect can be eliminated in Advance LIGO interferometer after the detailed experimental investigations supported by theoretical analysis.

Acknowledgments

We are grateful to Farid Khalili, David Ottaway, David Shoemaker, Ken Strain, Beno Willke, Bill Kells and Chunnong Zhao for valuable notes. This work was supported by LIGO team from Caltech and in part by NSF and Caltech grant PHY-0353775, by the Russian Agency of Industry and Science, contracts No. 5178.2006.2 and 02.445.11.7423.

APPENDIX A: FP CAVITY WITH TWO MOVABLE MIRRORS

Here we derive formulas (2.1, 2.2) and also obtain the equations describing opto-elastic coupling in FP cavity with two movable mirrors (see notations in fig. 3).

We denote distance between FP cavities mirrors as L . Close to resonance case it is convenient to introduce “generalized transparency” \mathcal{T}_Ω and “generalized reflectivity” \mathcal{R}_Ω for Stokes mode (2.3) using the following approximation:

$$\theta = e^{i(\omega_1 + \Omega)\tau} \simeq 1 + i\Omega\tau, \quad \tau = \frac{L}{c}.$$

Close to resonance we use the following approximation $\Omega\tau \ll 1$, $T \ll 1$.

The mean amplitude of main mode falling on end mirror is \mathcal{F}_{in} and we assume it as a constant.

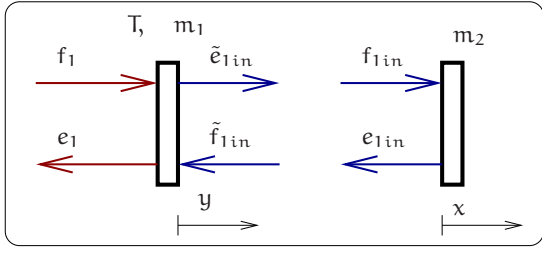


FIG. 3: Scheme of FP cavity and notations. Both mirrors can move as free masses.

In general case for fields on end mirror we have

$$\sum_n \frac{\mathcal{A}_{1in}^{(n)}}{\sqrt{S_1^{(n)}}} e_{1in}^{(n)} e^{-i\omega_1 t} = - \sum_n \frac{\mathcal{A}_{1in}^{(n)}}{\sqrt{S_1^{(n)}}} f_{1in}^{(n)} e^{-i\omega_1 t} - \frac{\mathcal{A}_{0in}}{\sqrt{S_0}} \mathcal{F}_{1in} e^{-i\omega_0 t} 2ik u_{\perp} (\chi e^{-i\omega_m t} + \chi^* e^{i\omega_m t}).$$

Here sum is taken over the complete set $\mathcal{A}_{1in}^{(n)}$ of cavity's modes (they are orthogonal to each other) and u_{\perp} is normal to surface component of displacement vector \vec{u} of elastic mode and χ is slow amplitude of displacement. Multiplying this equation by distribution function \mathcal{A}_{1in}^* of our Stokes mode, integrating over cross section and omitting non-resonance term ($\sim \chi e^{-i\omega_m t}$) one can find in frequency domain

$$e_{1in}(\Omega) = -f_{1in}(\Omega) - N_1 \mathcal{F}_{1in} 2ik \chi^* (\Delta - \Omega), \quad (A1)$$

$$N_1 = \frac{\int \mathcal{A}_{0in} \mathcal{A}_{1in}^* u_{\perp} d\vec{r}_{\perp}}{\sqrt{S_0 S_1}}. \quad (A2)$$

For fields on input mirror we have (see notations in fig. 3)

$$\tilde{e}_{1in} = iT f_1 - R \tilde{f}_{1in} + R(-\mathcal{F}_{1in}) N_1 2iky^*, \quad (A3)$$

$$e_1 = iT \tilde{f}_{1in} - R f_1 - R N_1 \mathcal{F}_{1in} 2i\omega_1 y^*/c, \quad (A4)$$

$$f_{1in} = \tilde{e}_{1in} \theta, \quad \tilde{f}_{1in} = \theta e_{1in}. \quad (A5)$$

Combining these equations one can obtain:

$$f_{1in} = \mathcal{T}_{\Omega} f_1 + \frac{N_1 \mathcal{F}_{1in} \mathcal{T}_{\Omega}}{iT} 2ik(\chi^* - y^*), \quad (A6)$$

$$f_{1in} \simeq \tilde{e}_{1in}, \quad \tilde{f}_{1in} \simeq e_{1in} = -\tilde{e}_{1in}, \quad (A7)$$

$$e_1 = f_1 \mathcal{R}_{\Omega} - N_1 \mathcal{F}_{1in} \mathcal{T}_{\Omega} 2ik(\chi^* - y^*). \quad (A8)$$

One can find equation for amplitude f_{1in} in time domain using the rule $(-i\Omega) \rightarrow \partial_t$:

$$\dot{f}_{1in} + \gamma f_{1in} = \frac{N_1 \mathcal{F}_{1in} \mathcal{T}_{\Omega}}{iT} 2ik(\chi^*(t) - y^*(t)) e^{-i\Delta t}. \quad (A9)$$

The light pressures acting on end mirror and input mirror inside the cavity are approximately equal to each other. So we can calculate light pressure acting only

on end mirror. Keeping only cross term we can obtain formula for light pressure P in time domain:

$$P \simeq \frac{2}{c\sqrt{S_0 S_1}} \left(\mathcal{A}_{0in} \mathcal{A}_{1in}^* \mathcal{F}_{1in} f_{1in}^*(t) e^{-i(\omega_0 - \omega_1)t} + \mathcal{A}_{0in}^* \mathcal{A}_{1in} \mathcal{F}_{1in}^* f_{1in}(t) e^{i(\omega_0 - \omega_1)t} \right).$$

Now we can write down equation for elastic oscillations with amplitude χ :

$$\rho \sum_{\ell} \vec{u}_{\ell} (\ddot{\chi}_{\ell} + 2\gamma_m^{(\ell)} \dot{\chi}_{\ell} + (\omega_m^{(\ell)})^2 \chi_{\ell}) = \vec{n}_{\perp} P(\vec{r}_{\perp}) \delta(r_{\parallel} - r_{\parallel}^0).$$

Here ρ is density of mirror, sum is taken over the complete set of elastic modes (spatial displacement vectors \vec{u}_{ℓ} are orthogonal to each other), \vec{n}_{\perp} is unit normal to mirror's surface, r_{\parallel} is longitudinal coordinate of points inside body of mirror, coordinate r_{\parallel}^0 corresponds to face surface of mirror. Multiplying this equation by spatial distribution vector \vec{u}^* of our elastic mode and integrating over mirror volume V one can obtain:

$$\ddot{\chi} + 2\gamma_m \dot{\chi} + \omega_m^2 \chi = \frac{2(N_1^* \mathcal{F}_{1in}^* f_{1in}(t) e^{i(\omega_0 - \omega_1)t} + \text{c.c.})}{cm\mu}, \quad (A10)$$

$$\mu = \frac{1}{V} \int |\vec{u}(\vec{r})|^2 d\vec{r},$$

where $m = \rho V$ is mirror's mass.

Introducing the slow amplitudes $\chi \Rightarrow \chi e^{-i\omega_m t} + \chi^* e^{i\omega_m t}$ we write down equation for amplitude χ^* :

$$\dot{\chi}^* + \gamma_m \chi^* = \frac{N_1^*}{icm\mu\omega_m} \mathcal{F}_{1in}^* f_{1in}(t) e^{i\Delta t}. \quad (A11)$$

And for the coordinate $z = x - y$ we finally obtain (if FP mirrors are elastically identical):

$$\dot{z}^* + \gamma_m z^* = \frac{2N_1^*}{icm\mu\omega_m} \mathcal{F}_{1in}^* f_{1in}(t) e^{i\Delta t}. \quad (A12)$$

APPENDIX B: SYMMETRIC MODE

In this Appendix we derive equations (2.9, 2.10) for analysis of parametric instability in symmetric mode. One can start from equations for amplitudes F_3 and E_3 on beam splitter:

$$F_3 e^{-i\phi_{pr}} = i\sqrt{T_{pr}} F_5 - \sqrt{1 - T_{pr}} E_3 e^{i\phi_{pr}}, \quad (B1)$$

$$E_5 = i\sqrt{T_{pr}} E_3 e^{i\phi_{pr}} - \sqrt{1 - T_{pr}} F_5, \quad (B2)$$

$$\phi_{pr} = (\omega_0 + \Delta_{pr} + \Omega) l_{pr}/c. \quad (B3)$$

We assume that PR cavity is in resonance: $\exp(i\phi_{pr}) = i$ and we assume that ϕ_{pr} does not depend on frequency Ω due to shortness of PR cavity ($l_{pr} \ll L$). Then using

(2.8) one can obtain:

$$f_3 \simeq \frac{\gamma - i\Omega}{(\gamma_{0+} - i\Omega)} \frac{-f_5 \sqrt{T_{pr}}}{1 + \sqrt{1 - T_{pr}}} - \frac{2\sqrt{2}\gamma \mathcal{F}_{1in} \sqrt{1 - T_{pr}} N_1 k z_+^*}{\sqrt{T}(1 + \sqrt{1 - T_{pr}})(\gamma_{0+} - i\Omega)}, \quad (B4)$$

$$e_5 = \frac{f_5(\gamma_{0+} + i\Omega)}{(\gamma_{0+} - i\Omega)} + \frac{\sqrt{T_{pr}} \mathcal{F}_{1in} \gamma 2\sqrt{2} N_1 k z_+^*}{\sqrt{T}(1 + \sqrt{1 - T_{pr}})(\gamma_{0+} - i\Omega)}, \quad (B5)$$

$$\gamma_{0+} = \gamma \frac{1 - \sqrt{1 - T_{pr}}}{1 + \sqrt{1 - T_{pr}}} \simeq \frac{T_{pr}\gamma}{4}. \quad (B6)$$

The fluctuation part f_+ of symmetric mode. We rewrite equation (2.1) using (2.5, B4):

$$f_{in+} = \frac{2i\sqrt{T_{pr}}\gamma f_5}{\sqrt{T}(1 + \sqrt{1 - T_{pr}})(\gamma_{0+} - i\Omega)} + \frac{\mathcal{F}_{1in} 2\sqrt{2}i\gamma k N_1 z_+^*}{T(\gamma_{0+} - i\Omega)}. \quad (B7)$$

Recall that in frequency domain we mean $z_+^* = z_+^*(\Delta - \Omega)$ (Δ is a detuning (2.4)).

Now we can write down Eq. (B7) in time domain using rule $-i\Omega \rightarrow \partial_t$:

$$(\partial_t + \gamma_{0+})f_{in+} = \frac{i\sqrt{T_{pr}}\gamma f_5}{\sqrt{T}} + \frac{2\sqrt{2}i\mathcal{F}_{1in} N_1 \gamma k z_+^*}{T}.$$

For analysis of parametric instability in last equation we omit term proportional to f_5 and finally obtain Eq. (2.9).

Then we can calculate the ponderomotive forces acting on each mirror and write equation for sum coordinate z_+ :

$$\frac{F_{pm+}}{m} = \ddot{z}_+ + 2\gamma_m \dot{z}_+ + \omega_m^2 z_+, \quad (B8)$$

$$F_{pm+} \simeq \frac{2\sqrt{2}N_1}{\pi} \left(\mathcal{F}_{1in} f_{in+}^*(t) e^{-i(\omega_0 - \omega_1)t} + \mathcal{F}_{1in}^* f_{in+}(t) e^{i(\omega_0 - \omega_1)t} \right). \quad (B9)$$

We rewrite (B9) keeping only resonance terms:

$$F_{pm+} \simeq \frac{2\sqrt{2}N_1}{\pi} \mathcal{F}_{1in}^* f_{in+}(t) e^{i(\omega_0 - \omega_1)t}, \quad (B10)$$

$$\frac{F_{pm+}}{2i\omega_m m} = e^{i\omega_m t} (\dot{z}_+^* + \gamma_m z_+^*). \quad (B11)$$

Now we can obtain equation (2.10).

APPENDIX C: ANTI-SYMMETRIC MODE

In this Appendix we derive equations (2.18, 2.19) for analysis of parametric instability in anti-symmetric

mode. For amplitudes F_4 and E_4 on beam splitter we have:

$$F_4 e^{-i\phi} = i\sqrt{T_{sr}} F_6 - \sqrt{1 - T_{pr}} E_4 e^{i\phi}, \quad (C1)$$

$$E_6 = i\sqrt{T_{sr}} E_4 e^{i\phi} - \sqrt{1 - T_{sr}} F_6. \quad (C2)$$

We assume that SR cavity is not in resonance (i.e. $\phi = (\omega_0 + \Omega)l_{sr}/c$ is an arbitrary number) and that ϕ does not depend on frequency Ω due to shortness of SR cavity ($l_{sr} \ll L$). Then using (2.7) one can obtain:

$$f_4 = \frac{if_6 \sqrt{T_{sr}} e^{i\phi} (\gamma - i\Omega)}{(1 + \sqrt{1 - T_{sr}} e^{2i\phi})(\gamma_{0-} - i(\delta + \Omega))} + \frac{2\sqrt{2}i\gamma e^{2i\phi} \sqrt{1 - T_{sr}} \mathcal{F}_{1in} N_1 k z_-^*}{\sqrt{T}(1 + \sqrt{1 - T_{sr}} e^{2i\phi})(\gamma_{0-} - i(\delta + \Omega))}, \quad (C3)$$

$$e_6 = \frac{f_6 e^{2i\phi} (\gamma_{0-} + i(\delta + \Omega))}{(\gamma_{0-} - i(\delta + \Omega))} + \frac{2\sqrt{2}\gamma \sqrt{T_{sr}} e^{i\phi} \mathcal{F}_{1in} N_1 k z_-^*}{\sqrt{T}(1 + \sqrt{1 - T_{sr}} e^{2i\phi})(\gamma_{0-} - i(\delta + \Omega))}, \quad (C4)$$

$$\delta = \frac{\gamma \sqrt{1 - T_{sr}} \sin 2\phi}{(1 - T_{sr}/2 + \sqrt{1 - T_{sr}} \cos 2\phi)}, \quad (C5)$$

$$\gamma_{0-} = \frac{\gamma T_{sr}}{2(1 - T_{sr}/2 + \sqrt{1 - T_{sr}} \cos 2\phi)}. \quad (C6)$$

We rewrite equation (2.1) using (2.6, C3) to obtain formula for fluctuation part f_- of anti-symmetric mode:

$$f_{in-} = \frac{2\gamma \sqrt{T_{sr}} f_6 e^{i\phi}}{\sqrt{T}(1 + \sqrt{1 - T_{sr}} e^{2i\phi})(\gamma_{0-} - i(\delta + \Omega))} + \frac{2\sqrt{2}i\gamma \mathcal{F}_{1in} N_1 k z_-^*}{T(\gamma_{0-} - i(\delta + \Omega))}. \quad (C7)$$

For analysis of parametric instability we can omit the term proportional to f_6 so that

$$f_{in-} = \frac{N_1 \mathcal{F}_{1in} i\omega_1 z_-^*}{L\sqrt{2}(\gamma_{0-} - i(\delta + \Omega))}. \quad (C8)$$

Finally one can obtain from (C8) the equation (2.18) in time domain.

In the same manner as for symmetric mode one can obtain the formula for ponderomotive force in anti-symmetric mode:

$$\frac{F_{pm-}}{m} = \ddot{z}_- + 2\gamma_m \dot{z}_- + \omega_m^2 z_-, \quad (C9)$$

$$F_{pm-} \simeq \frac{2\sqrt{2}S}{\pi} \left(\mathcal{F}_{1in} f_{in-}^*(t) e^{-i(\omega_0 - \omega_1)t} + \mathcal{F}_{1in}^* f_{in-}(t) e^{i(\omega_0 - \omega_1)t} \right). \quad (C10)$$

Keeping only resonance terms and rewriting (C9,C10) one can obtain equation (2.19) for differential coordinate z_- in time domain.

APPENDIX D: ONLY ONE MIRROR IS IN RESONANCE

For ponderomotive force we have

$$\begin{aligned} F_{\text{pm}} &= \frac{2S(E_{\text{main}} + E_{\text{Stokes}})^2}{4\pi} \simeq \\ &\simeq \frac{2}{c\mu} (N_1 \mathcal{F}_{1\text{in}}(t) f_{1\text{in}}^*(t) + N_1^* \mathcal{F}_{1\text{in}}^*(t) f_{1\text{in}}(t)). \end{aligned} \quad (\text{D1})$$

Keeping only resonance term ($\sim f_{1\text{in}}$) we obtain equation for elastic mode:

$$\dot{x}_1^* + \gamma_m x_1^* = \frac{N_1^* \mathcal{F}_{1\text{in}}^* e^{i\Delta t}}{ic\mu m\omega_m} f_{1\text{in}}(t), \quad \Delta = \omega_0 - \omega_1 - \omega_m.$$

Taking into account both anti-symmetric and symmetric modes we finally obtain the set of equations in time domain:

$$\dot{x}_1^* + \gamma_m x_1^* - \frac{N_1^* \mathcal{F}_{1\text{in}}^*}{ic\mu m\omega_m} \frac{f_{1\text{in}+} + f_{1\text{in}-}}{\sqrt{2}} e^{i\Delta t} = 0, \quad (\text{D2})$$

$$-\frac{iN_1 \mathcal{F}_{1\text{in}} \omega_1}{\sqrt{2}L} x_1^* e^{-i\Delta t} + (\partial_t + \gamma_{0+}) f_{1\text{in}+} = 0, \quad (\text{D3})$$

$$-\frac{iN_1 \mathcal{F}_{1\text{in}} \omega_1}{\sqrt{2}L} x_1^* e^{-i\Delta t} + (\partial_t - i\delta + \gamma_{0-}) f_{1\text{in}-} = 0. \quad (\text{D4})$$

We sum and subtract equations (D3, D4) (see also definitions (2.5, 2.6)):

$$\dot{f}_{1\text{in}+} + \frac{\gamma_{0+} + \Gamma_{0-}}{2} f_{1\text{in}+} + \frac{\gamma_{0+} - \Gamma_{0-}}{2} f_{2\text{in}} = \sigma, \quad (\text{D5})$$

$$\dot{f}_{2\text{in}} + \frac{\gamma_{0+} + \Gamma_{0-}}{2} f_{2\text{in}} + \frac{\gamma_{0+} - \Gamma_{0-}}{2} f_{1\text{in}} = 0, \quad (\text{D6})$$

where we introduced notations:

$$\sigma \equiv \frac{iN_1 \mathcal{F}_{1\text{in}} \omega_1}{L} x_1^* e^{-i\Delta t}, \quad \Gamma_{0-} \equiv \gamma_{0-} - i\delta.$$

Manipulating Eqs. (D5, D6) we get:

$$\left(\partial_t + \frac{\gamma_{0+} + \Gamma_{0-}}{2} \right) \times (\text{D5}) - \left(\frac{\gamma_{0+} - \Gamma_{0-}}{2} \right) \times (\text{D6}) :$$

$$\ddot{f}_{1\text{in}+} + (\gamma_{0+} + \Gamma_{0-}) \dot{f}_{1\text{in}+} + \gamma_{0+} \Gamma_{0-} f_{1\text{in}+} = \dot{\sigma} + \frac{\gamma_{0+} + \Gamma_{0-}}{2} \sigma.$$

Finally we have the set of equations:

$$\dot{x}_1^* + \gamma_m x_1^* - \frac{N_1^* \mathcal{F}_{1\text{in}}^*}{ic\mu m\omega_m} f_{1\text{in}}(t) e^{i\Delta t} = 0, \quad (\text{D7})$$

$$\frac{-iN_1 \mathcal{F}_{1\text{in}} \omega_1}{L} \left(\partial_t + \frac{\gamma_{0+} + \Gamma_{0-}}{2} \right) x_1^* e^{-i\Delta t} +$$

$$+\ddot{f}_{1\text{in}+} + (\gamma_{0+} + \Gamma_{0-}) \dot{f}_{1\text{in}+} + \gamma_{0+} \Gamma_{0-} f_{1\text{in}+} = 0.$$

Finding the solution of this set in form: $f_{1\text{in}}(t) = f_{1\text{in}} e^{\lambda t}$, $x_1^*(t) = x_1^* e^{(\lambda + i\Delta)t}$ we obtain characteristic equation:

$$\frac{(\lambda + i\Delta + \gamma_m)(\lambda + \gamma_{0+})(\lambda + \Gamma_{0-})}{(2\lambda + \gamma_{0+} + \Gamma_{0-})} = \frac{Q}{2}.$$

Using this equation we get Eq. (2.25).

The instability condition for pure SR configuration. As before we substitute $\lambda = \mathbf{a} + i(\mathbf{b} - \Delta)$ into (2.25) taking $\mathbf{a} = 0$:

$$\gamma_m = \underbrace{\gamma_{0+} A_1}_{\gamma_{m1}} + \underbrace{\gamma_{0-} A_2}_{\gamma_{m2}}, \quad (\text{D9})$$

$$\mathbf{b} = A_1(\Delta - \mathbf{b}) + A_2(\Delta + \delta - \mathbf{b}). \quad (\text{D10})$$

Here we introduce notations

$$A_1 = \frac{Q}{2} \frac{1}{\gamma_{0+}^2 + (\mathbf{b} - \Delta)^2}, \quad \gamma_{m1} = \gamma_{0+} A_1, \quad (\text{D11})$$

$$A_2 = \frac{Q}{2} \frac{1}{\gamma_{0-}^2 + (\mathbf{b} - \Delta - \delta)^2}, \quad \gamma_{m2} = \gamma_{0-} A_2. \quad (\text{D12})$$

We can formally solve Eq. (D10) and find \mathbf{b} :

$$\mathbf{b} = \frac{\frac{\gamma_{m1}}{\gamma_{0+}} \Delta + \frac{\gamma_{m2}}{\gamma_{0-}} (\Delta + \delta)}{1 + \frac{\gamma_{m1}}{\gamma_{0+}} + \frac{\gamma_{m2}}{\gamma_{0-}}}. \quad (\text{D13})$$

Note that values γ_{m1} and γ_{m2} in (D9) are positive ones and hence $\gamma_{m1}, \gamma_{m2} < \gamma_m$. Also taking into account that $\gamma_{m1}, \gamma_{m2} \ll \gamma_{0+}, \gamma_{0-}$ we can conclude from (D13) that

$$\mathbf{b} \ll |\Delta|, |\Delta + \delta|. \quad (\text{D14})$$

Then the parametric instability condition (2.30) can be easily obtained from Eq. (D9) using inequality (D14).

APPENDIX E: NUMERICAL PARAMETERS

We used the parameters planned for Advanced LIGO [5]:

$$\begin{aligned} \omega_0 \simeq \omega_1 &\simeq 2 \times 10^{15} \text{ sec}^{-1}, & L &= 4 \times 10^5 \text{ cm}, \\ m &= 40 \text{ kg}, & W &= 830 \text{ kW}, \\ T &= 5 \times 10^{-3}, & T_{\text{pr}} &= 6 \times 10^{-2}, \\ \gamma &\simeq 94 \text{ sec}^{-1}, & \gamma_{0+} &\simeq 1.5 \text{ sec}^{-1}, \\ T_{\text{sr}} &= 7 \times 10^{-2}. \end{aligned}$$

We also assume that FP mirrors are fabricated from fused silica with angle of structural losses $\phi = 1.2 \times 10^{-8}$ and for elastic modes frequencies $\omega_m = 10^5 \div 10^7 \text{ sec}^{-1}$ we estimate relaxation rate γ_m of elastic modes by formula:

$$\gamma_m = \omega_m \phi / 2 \simeq 6 \times (10^{-4} \div 10^{-2}) \text{ sec}^{-1}.$$

-
- [1] A. Abramovici *et al.*, *Science* **256**, 325 (1992).
- [2] A. Abramovici *et al.*, *Physics Letters* **A218**, 157 (1996).
- [3] LIGO technical document G060052-00-E; current sensitivity curves are available on http://www.ligo.caltech.edu/~lazz/distribution/LSC_Data/.
- [4] Advanced LIGO System Design (LIGO-T010075-00-D), Advanced LIGO System requirements (LIGO-G010242-00), available in <http://www.ligo.caltech.edu> .
- [5] <http://www.ligo.caltech.edu/~ligo2/scripts/12refdes.htm>
- [6] V. B. Braginsky, S. E. Strigin, and S. P. Vyatchanin, *Physics Letters* **A287**, 331 (2001); gr-qc/0107079.
- [7] E. D'Ambrosio and W. Kells, *Physics Letter* **A299**, 326 (2002). LIGO-T020008-00-D, available in <http://www.ligo.caltech.edu>.
- [8] V. B. Braginsky, S. E. Strigin and S. P. Vyatchanin, *Physics Letters* **A305**, 111 (2002).
- [9] V. B. Braginsky and S. P. Vyatchanin, *Physics Letters* **A293**, 228 (2002).
- [10] T. Corbitt, D. Ottaway, E. Innerhofer, J. Pelc, and N. Mavalvala, accepted to *Phys.Rev.A*
- [11] C. Zhao, L. Ju, J. Degallaix, S. Gras, and D. G. Blair, *Phys. Rev. Lett.* **94**, 121102 (2005).
- [12] L. Ju, S. Gras, C. Zhao, J. Degallaix and D. G. Blair, *Phys. Lett.* **A354**, 360 (2006).
- [13] L. Ju, C. Zhao, S. Gras, J. Degallaix, D. G. Blair, J. Munch and D. H. Reitze, *Phys. Lett. A*, accepted (2006).
- [14] T. J. Kippenberg, H. Rokhsari, T. Carmon, A. Scherer, and K. J. Vahala, *Phys. Rev. Lett.* **95**, 033901, July 2005.
- [15] H. Rokhsari, T. J. Kippenberg, T. Carmon, and K. J. Vahala, *Optics express* **13**, 5293 (2005).
- [16] K. Thorne, private communication.
- [17] P. Savov, K. Thorne, S P. Vyatchanin, LIGO document G050441-00-Z, available in <http://www.ligo.caltech.edu> .
- [18] P. Savov, K. Thorne, work in progress.